Zeitschrift: IABSE proceedings = Mémoires AIPC = IVBH Abhandlungen
Band: 10 (1986)
Heft: P-98: Dynamic factor of highway steel girder bridges

Artikel: Dynamic factor of highway steel girder bridges
Autor: Honda, Hideyuki / Kobori, Tameo / Yamada, Yoshikazu
DOI: https://doi.org/10.5169/seals-39607

Dynamic Factor of Highway Steel Girder Bridges

Facteur dynamique pour des ponts-routes métalliques

Stosszuschlag für stählerne Strassenbrücken

Hideyuki HONDA
Assoc. Prof.
Kanazawa Inst. of Technol.
Kanazawa, Japan

Tameo KOBORI
Prof. Dr.
Kanazawa University
Kanazawa, Japan

Yoshikazu YAMADA
Prof. Dr.
Kyoto University
Kyoto, Japan

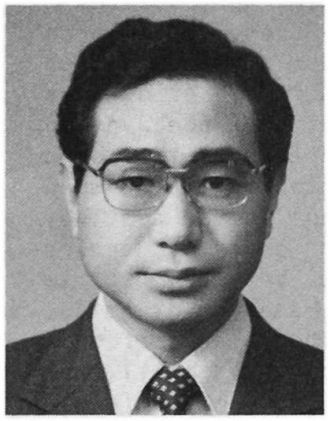

Hideyuki Honda, born 1950, obtained the degree of Doctor of Engineering at Kyoto Univ. He is researching the dynamic effects of highway bridges under moving vehicles.

Tameo Kobori, born 1930, obtained the degree of Doctor of Engineering at Kyoto Univ. Since 1971, he has been a professor of structural engineering at Kanazawa University.

Yoshikazu Yamada, born 1929, obtained the degree of Doctor of Engineering at Kyoto Univ. Since 1961 he has been a professor of structural and earthquake engineering at Kyoto Univ.

SUMMARY

The dynamic behavior of highway steel girder bridges under moving vehicles is analyzed. Numerical examples are presented to show the dynamic effects of single-span bridges and of multi-span continuous bridges. The dynamic factor based on the deflection and the bending moment of the highway bridges, including both single-span and multi-span continuous bridges, is presented as a decreasing function with two parameters: the span length and the number of spans.

RÉSUMÉ

Le comportement dynamique de ponts-routes métalliques sous l'effet de charges mobiles fait l'objet de cette étude. Des exemples numériques montrent les effets dynamiques pour des ponts d'une ou plusieurs travées. Le facteur dynamique basé sur la déformation et le moment fléchissant des ponts-routes, à une ou plusieurs travées, est une fonction décroissante à deux paramètres, la longueur et le nombre des travées.

ZUSAMMENFASSUNG

Das dynamische Verhalten von Strassenbrücken aus Stahl mit einer oder mehreren Spannweiten wird anhand numerischer Beispiele untersucht. Der aus Durchbiegung und Biegemomenten ermittelte Stosszuschlag für Strassenbrücken nimmt mit steigenden Spannweiten und zunehmender Felderzahl ab.

1. INTRODUCTION

A variety of technical problems related to highway bridges have arisen in recent years due to the increasing number of heavy trucks on highways. The problem of the dynamic behavior of highway bridges due to live loads must be investigated in order to determine the most efficient method of designing bridges. The dynamic behavior problem is included in the problem of the impact on highway bridges of moving vehicles. However, the dynamic behavior of highway bridges under moving vehicles is affected greatly by various factors such as the characteristics of vehicles, the road surface roughness and the bridges. It is difficult to account for all these factors in the design of bridges. For simplicity and practical application, all these factors contributing to the dynamic behavior are customarily refered to the word "impact".

Various studies on such impact problem of highway bridges have been undertaken, and important data have been reported. However, most of those studies have been done on single-span bridges, and there has been comparatively little attention given to the behavior of multi-span continuous bridges. The stress caused by a live load on long span highway bridges is generally smaller than that caused by dead load. In addition, the dynamic behavior on a long span bridge due to this live load differs from that on a short span bridge. However, at present, the impact factor of multi-span continuous bridges, one type of long span bridge, is treated in the same way as the impact factor on single-span bridges. Therefore, in order to develop an efficient method of designing multi-span continuous bridges, it is necessary to investigate the impact factor of these bridges based on dynamics. In addition, it is absolutely essential to investigate the different characteristics of the dynamic behavior between single-span and multi-span continuous bridges, and it is absolutely essential to develop an impact factor which is appropriate for both types of bridge.

It is preferable to use the bending moment rather than the deflection in the investigation of the impact factor, because the expression of the impact factor indicated in the design specifications is used to mean the dynamic effect of the maximum stress caused by the design live load. Although the impact factor based on response deflection has been studied at some length, there has been comparatively little attention given to the impact factor based on response bending moment, because the impact factor adopted in current design specifications is based on the relation between the span length and the amplitude of dynamic deflection determined by vibration tests of actual bridges. However, when the impact factor used in design is tested by a vibration test on actual bridges, the response deflection is also measured, because the response strain of each bridge member is too small to measure. In theoretical and experimental investigations of the impact factor, there is also reason to measure the response deflection. Therefore, it is necessary to investigate both impact factors based on the response both of the bending moment and the deflection.

The object of this study is three-fold: (1) To investigate the dynamic behavior of single-span bridges and multi-span continuous bridges, (2) To estimate the magnitude of the dynamic factor of the two types of highway steel girder bridges, and (3) To give explicitly the decreasing function of the dynamic factor with two parameters: the span length and the number of spans of the highway bridge from the results of (2).

In this study the dynamic effect of highway bridges under moving vehicles is termed the "dynamic factor", and is distinguished from the "impact factor" found in current design specifications.

2. ANALYTICAL PROCEDURE

2.1 Equation of motion on vehicle-bridge system

Fig.1 shows the vibrational model of the vehicle-bridge system. Using the generalized coordinate, $q_n(t)$, and the vibration mode function, $\phi_n(x)$, the deflection of the bridge in Fig.1 is given by the modal analysis method as

$$y(t,x) = \sum_{n=1}^{\infty} q_n(t)\ \phi_n(x) \qquad (1)$$

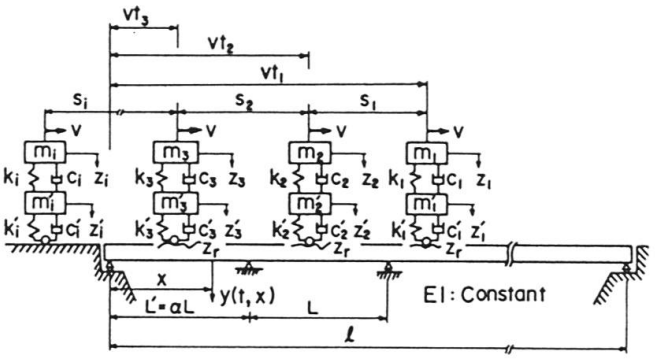

Fig.1 Vehicle-bridge system.

The mode function, $\phi_n(x)$, is defined by a series as

$$\phi_n(x) = \sum_{m=1}^{\infty} a_{nm} \sin\frac{m\pi x}{l} \qquad (2)$$

$$\sum_{m=1}^{\infty} a_{nm}^2 = \frac{2}{\rho l} \qquad (3)$$

Using the total span length, l, and the bridge mass, ρ, per unit span length, the parameter, a_{nm}, is normalized by Eq.(3).

The equations of motion of the vehicle-bridge system are obtained by an energy method as

$$\ddot{q}_n(t) + 2h_n\omega_n\dot{q}_n(t) + \omega_n^2 q_n(t) = \sum_{i=1}^{n} \frac{2gR_i}{R_i'}\gamma_i\left[\{\mu_i'(z_i'-y_i) + \nu_i(\dot{z}_i'-\dot{y}_i) + (R_i'+1)\}\right]\phi_n(Vt_i) \qquad (4)$$

$$\ddot{z}_i + g\{\mu_i(z_i-z_i') + \nu_i(\dot{z}_i-\dot{z}_i')\} = 0 \qquad (5)$$

$$\ddot{z}_i' + R_i'g\{\mu_i(z_i'-z_i) + \nu_i(\dot{z}_i'-\dot{z}_i)\} + g\{\mu_i'(z_i'-y_i) + \nu_i'(\dot{z}_i'-\dot{y}_i)\} = 0 \qquad (6)$$

where,

$$\left.\begin{aligned} R_i &= m_i/(\rho l), \quad R_i' = m_i/m_i' \\ \mu_i &= k_i/(m_i g), \quad \mu_i' = k_i'/(m_i' g) \\ \nu_i &= c_i/(m_i g), \quad \nu_i' = c_i'/(m_i' g) \end{aligned}\right\} \qquad (7)$$

$$y_i = y(t,x) + z_r(x_i) \qquad (8)$$

The bending moment, $M(t,x)$, is given in the form of the following differentiation,

$$M(t,x) = -EI \frac{\partial^2 y(t,x)}{\partial x^2} = EI \sum_{n=1}^{\infty} q_n(t) \sum_{m=1}^{\infty} \left(\frac{m\pi}{l}\right)^2 a_{nm} \sin\frac{m\pi x}{l} \quad (9)$$

2.2 Definition of dynamic factor

In much the same manner used in present design specification of bridges, the dynamic factor in this study is calculated at each span and at intermediate supports. The dynamic factors, i_y and i_M, based on deflection and bending moment are defined as

$$i_y = (y_{d,max} - y_{s,max}) / y_{s,max} \quad (10)$$

$$i_M = (M_{d,max} - M_{s,max}) / M_{s,max} \quad (11)$$

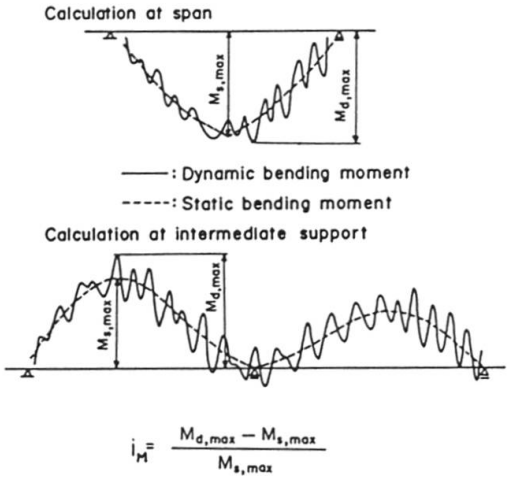

Fig.2 Dynamic factor based on bending moment.

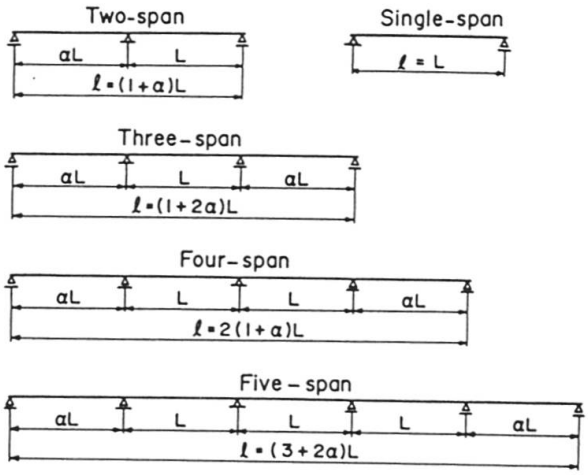

Fig.3 Bridge types.

Table 1 Design specifications of bridge types under study.

1	Bridge class	Bridge of class=1 (TL-20; TL-196 kN)							
2	Road width	Effective road width = 10 m							
3	Number of span	1	2	3	4	5			
4	Span length L (m)	20	30	40	50	60	70	80	90
5	Span ratio α	0.5	0.6	0.7	0.8	0.9	1.0		
6	Number of main girder	4							
7	Distance of main girder	3 m							
8	Height of web plate	h_w = L/22 (m); Constant height							
9 Dead load	Slab Pavement Weight of girder* The rest	RC slab (thickness = 0.22 m) Asphalt (thickness = 0.05 m) L/2.45 (kN/m); per unit road width 10 m Hand rail = 0.392 kN/m, Coping = 1.842 kN/m, Haunch = 0.98 kN/m							
10 Live load	Centered load Distributed load Impact factor	49 kN/m to direction of road width $L', L \leq 80$ m 3.45 kN/m^2, $80 < L', L \leq 130$ m (4.214-L',L) kN/m^2 L; i = 20/(50 + L), L' = αL ; i = 20/(50 + L')							
11	Used steel	SM 53; tensile strength = range of 519.4 to 637 MPa							

* : This weight of girder is the assumed weight calculated from various design examples.

As an example, Fig.2 shows the dynamic factor based on the bending moment. However, when the dynamic factor based on the response deflection of continuous girder bridges is investigated by Eq.(10), the dynamic factor at intermediate supports cannot be calculated because the deflection at such supports is zero.

2.3 Characteristics of bridges and vehicles considered

Two hundred bridges were investigated. The bridges are single-span, or multi-span continuous with two, three, four or five-spans (Fig.3). These 200 bridges were designed according to the design specifications shown in Table 1. The multi-span continuous bridges were designed as non-composite steel girder bridges, but the single-span bridges were designed as composite steel girder bridges.

The dynamic characteristics of these bridges were calculated using Hirai's method {1}. The frequency equation of continuous girder bridges is generally given as

$$\begin{vmatrix} C_{11}, & C_{12}, & \cdots\cdots\cdots, & C_{1n} \\ C_{21}, & C_{22}, & \cdots\cdots\cdots, & C_{2n} \\ \cdots\cdots\cdots\cdots\cdots\cdots\cdots\cdots & & & \\ C_{n1}, & C_{n2}, & \cdots\cdots\cdots, & C_{nn} \end{vmatrix} = 0 \qquad (12)$$

where,

$$\left.\begin{aligned} C_{ij} &= \sum_{m=1}^{\infty} \frac{1}{\omega_{gm}^2 - \omega_n^2} \sin\frac{m\pi x_i}{l} \sin\frac{m\pi x_j}{l} \\ \omega_{gm} &= (m\pi/l)^2 \sqrt{EI/\rho} \\ \omega_n &= \lambda_n (\pi/l)^2 \sqrt{EI/\rho} = \lambda_n \omega_{g1} \end{aligned}\right\} \qquad (13)$$

When λ_n is calculated by Eq(13), $\phi_n(x)$ which correcponds to ω_n can be obtained from Eq(12). The damping constant, h_n, of bridges was given the general value of 0.02 {2}.

Table 2 shows the properties of a vehicle with the natural frequencies of 3.1 Hz for sprung mass and 13.0 Hz for unsprung mass {3}. The vehicle is normalized for 196 kN(γ_i = 1.0 in Eq.4) which is the design live load according to the current specifications. The speed of the vehicle, V, need not be high, because the L-20 (L-196 kN) load vehicle load is assumed to be the fully loaded condition for each span of the bridge as explained below in Fig.7. Therefore, this speed is assigned the value of 10 m/s.

Table 2 Properties of hypothetical vehicle.

Speed (V) : 10 m/s	
Vehicle weight : 196 kN (sprung; 176.4 kN, unsprung; 19.6 kN)	
Spring stiffness	k_i = 6830.6 kN/m k_i' = 13328.0 kN/m
Damping factor	c_i = 24.5 kN/(m·s^{-1}) c_i' = 29.4 kN/(m·s^{-1})

2.4 Sample function of road surface roughness

The road surface roughness has been considered a cause of bridge vibration under moving vehicles. This roughness is expressed generally by a power spectral density (PSD) which is assumed from a stationary probability process with a zero mean value. The PSD, $S_r(\Omega)$, of road surface roughness is given

by the authors {4} as

$$S_r(\Omega) = a\ \Omega^{-n} \qquad (14)$$

The road surface roughness was measured by a surveyor's level, and then PSD was calculated by a maximum entropy method (MEM) {5,6}. The PSD of road surface roughness is shown by the bold solid line in Fig.4. This PSD indicates the mean spectrum of eighty four lines on 56 bridges based on the authors's investigation {4}. Using this PSD, the sample function of road surface roughness is calculated by Monte Carlo simulation {7} as

$$z_r(t) = \sigma \sqrt{2/N} \sum_{j=1}^{N} \cos(\Omega_j t + \phi_j) \qquad (15)$$

where,

$$\sigma = \sqrt{\int_{-\infty}^{\infty} S_r(\Omega)\ d\Omega}$$

Fig.5 shows a numerical example of the sample function.

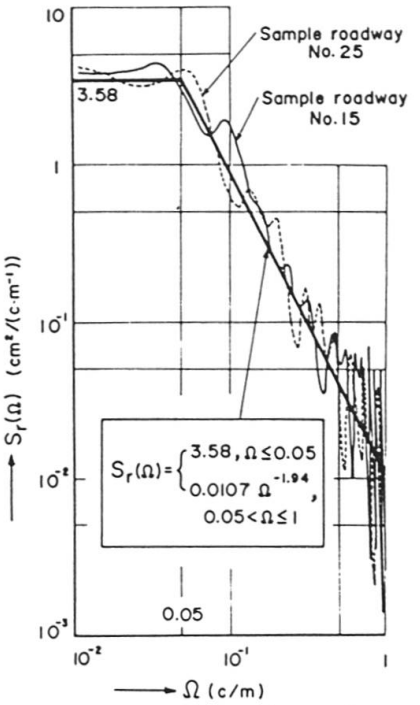

Fig.4 PSD of road surface roughness.

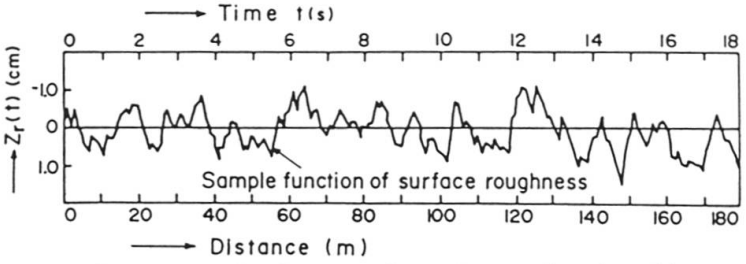

Fig.5 A numerical example of sample function (sample roadway No.15).

With the method of analysis used in this study, the number of the sample functions becomes a problem. To decide the number of sample functions to use, dynamic response analysis was done on the three-span continuous girder bridge (α = 1.0), varying the span length and the number of the sample functions, and then the maximum values of the dynamic bending moment at the center of the mid-span under a moving vehicle were calculated. The number of sample functions which produces mean value of maximum values which are least affected by variations in span length was determined. The optimum number of sample functions was thirty, and this number was adopted for this study. In addition, a spectrum analysis of these sample functions was done by MEM, and the calculated examples are indicated by the fine solid and the dotted line in Fig.4.

2.5 Initial condition of moving vehicle

When the vehicle passes over an expansion joint point, the momentary impact of the vehicle arises due to the roughness of the joint point. The vehicle vibration in this case is dominated by the vibration of the unsprung mass {7}. Therefore, the initial condition of the vehicle is represented by the vertical velocity, $\dot{z}_i'(t_0^*)$, of the unsprung mass at time t_0^* of instant of passing the joint point {8}, and it is given as

$$\dot{z}_i'(t_0^*) = \dot{z}_i'(t_0) + k_i'/m_i'\ A \int_{t_0}^{t_0^*} \delta(t)\,dt \qquad (16)$$

To decide the value of A, the author measured the roughness of two hundred and forty eight joint points on 91 bridges {9}. (three-meter sections of bridge surface including the joint point were measured.) Using this roughness data, the maximum value of $\dot{z}_i(t_0^*)$, produced by the unsprung mass of the vehicle

of Table 2 while passing the joint point in time t_0 to t_0^*, was calculated at each joint point. The set of these maximum values was considered to be a normal distribution, and then parameter A, which was the mean value plus 2 times the standard deviation of these maximum values, was calculated as the upper-limit value produced at the joint point in normal load conditions. Finally, in this study the fixed value of A = 0.0195 cm/s was adopted.

2.6 Numerical calculation

The equations of motion of Eqs.(4), (5) and (6) are calculated by Newmark's β method with β = 1/6. The time interval of the integration is assigned the value of 0.01 sec. based on the shortest natural period of the designed bridges, and the response deflection and bending moment are calculated by Eq.(1) and Eq.(9). Moreover, the place where the influence value of static response of bridges is the largest is chosen for the numerical calculation.

To decide the number n and m of each harmonic series of natural frequency and the vibrational mode of the multi-span continuous bridges, the maximum value of the dynamic bending moment of the multi-span continuous girder bridges under a moving vehicle was calculated. Table 3 shows an example of these calculated results. As the natural frequency of heavy vehicles is generally in the region of 2-4 Hz for sprung mass {10}, in single-span, two and three-span continuous bridges, n is taken to the 4-th frequencies, and is taken to the 6-th in four and five-span continuous bridges. The values in Table 3 are nomalized according to the maximum value of the dynamic bending moment at n = 4 and m = 6 or at n = 6 and m = 10. It was recognized that the effect of m on these maximum values is small. Therefore, in two and three-span continuous bridges, m is adopted to the 6-th terms, and it is adopted to the 10-th in four and five-span continuous bridges.

Table 3 Comparison of response bending moment by m.

Types	n	m			
		6	10	14	16
Two-span	4	1.000	1.005	1.050	1.064
Three-span	4	1.000	1.010	1.014	1.015
Four-span	6	—	1.000	1.002	1.039
Five-span	6	—	1.000	1.031	1.048

L=40 m, α=1.0, x=0.42αL, Sample roadway No. 15

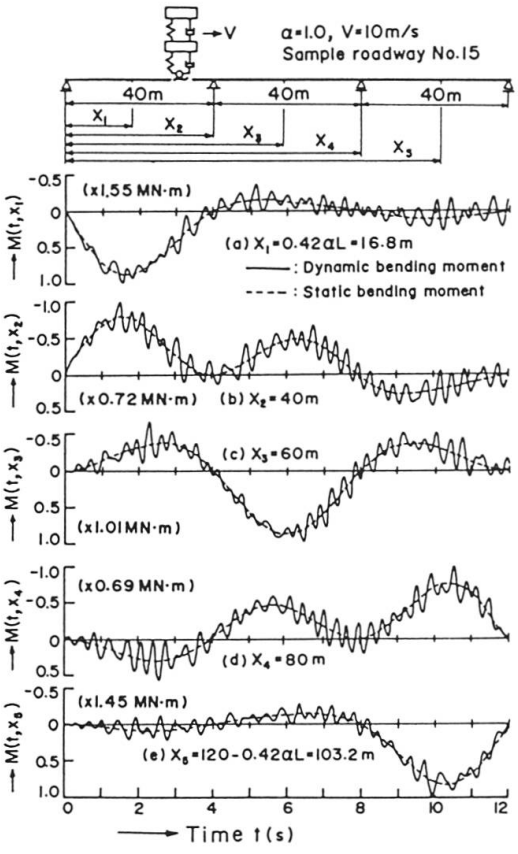

Fig.6 Response bending moment of three-span continuous girder bridge under a moving vehicle.

As a numerical example, Fig.6 shows the response bending moment at each point of calculation of the three-span continuous girder bridge under a moving vehicle. The solid line shows the dynamic bending moment, and the dotted line shows the static bending moment under the influence of the static load of the vehicle, $2gR_i\gamma_i(1+1/R_i')$, found on the right side of Eq.(4).

3. RESPONSE ANALYSIS UNDER EQUIVALENT VEHICLE LOAD LINE

3.1 Equivalent vehicle load line

To investigate the impact factor, it is most practical and useful to base analysis on the design live load. Therefore, the vehicle load line, which is equivalent to the design live load (L-20; L-196 kN) is assigned one load of 196 kN and other loads of 147 kN at 14 m intervals as shown in Fig.7. The number of vehicles is chosen so as to make the difference of strength between the defined load line and the design live load as small as possible. When this number is odd, the 196 kN vehicle is arranged at the center in this load line. When the number is even, it is arranged at the position where the response of the bridge is the largest before and after the mid point of the load line.

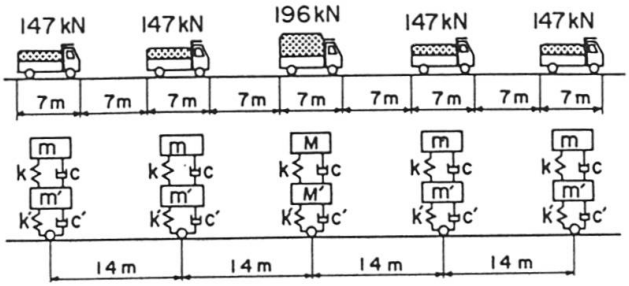

Fig.7 Hypothetical vehicle load line equivalent to design live load.

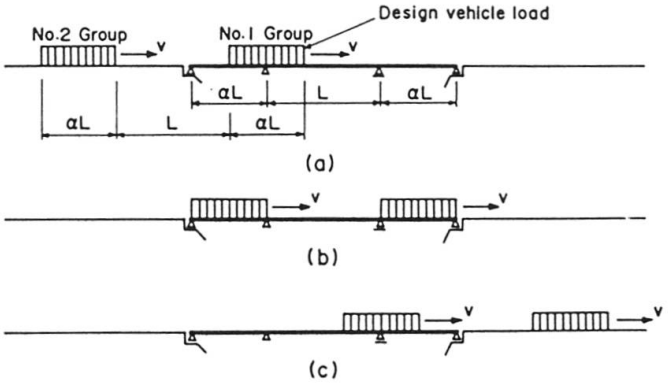

Fig.8 Example of moving vehicle load line groups on three-span continuous bridge (both side span loaded).

When the dynamic response of continuous girder bridges for practical traffic loads is analyzed, the vehicle load line shown in Fig.7 may be generally applied to the whole span. However, when the bending moment, which is used in design of the girder section, is calculated, the design live load is applied only to spans where the influence value of the bending moment has the same sign (positive or negative), and it is not applied to spans with the opposite sign. Therefore, in this study the movement of the vehicle load is investigated by the same method as that described for design live load. As an example, Fig.8 shows the movement of the vehicle load on a three-span continuous bridge. In regard to the side span loading, the vehicle load line defined as two groups of vehicles (Fig. 8), which would result in the fully loaded condition for both left and right side spans, is considered as in Fig.8(a). The interval between the two vehicle groups is chosen to correspond to mid-span length. When the head vehicle of group No.1 moves to the right end support as in Fig.8(b), the vehicle loads are applied to both side spans and are not applied to the mid span. The maximum value of the response of the bridge at the point of calculation on the side span is obtained by this loading condition. In regard to mid-span loading, the vehicle loads are applied to mid-span only, and are not applied to either side span. The maximum value of the mid-span center is then obtained.

3.2 Dynamic factor of single-span steel girder bridges

Fig.9 shows the relationship between the span length, L , and the dynamic factor, i_y , based on the deflection of single-span bridges under the vehicle load line illustrated in Fig.7. ○ is the average value of i_y which was calculated by Eq.(10) using the thirty sample functions of road surface

roughness; σ is the standard deviation of i_y; and the dotted area is i_y which ranges from the average value plus σ to the average value minus σ. For example, the value of 75% calculated at L = 40 m is included in this range. Two trends can be seen from Fig.9. The first is that the values of i_y in the dotted area decrease according to the increase of span length. It may be seen that in spite of the fact that the static deflection of bridges grows larger with the increase of the number of vehicles, the dynamic deflection amplitude does not increase as much as the static deflection because of the effect of the vibration phase and the dynamic damping effect of each vehicle. The second is that, as the span length increases, the standard deviation decreases, but it is greatest at L = 20 m because the vehicle moves separately and such short span bridges are greatly affected by the vehicle load. It can be seen that the effect of the road surface roughness on the dynamic deflection amplitude becomes smaller with the increase of the span length and the increase of the number of vehicles. Finally, when the dynamic factor of the bridge under the equivalent vehicle load line was investigated, it was demonstrated that the effect of the vehicle load on the dynamic factor becomes smaller with the increase of the span length.

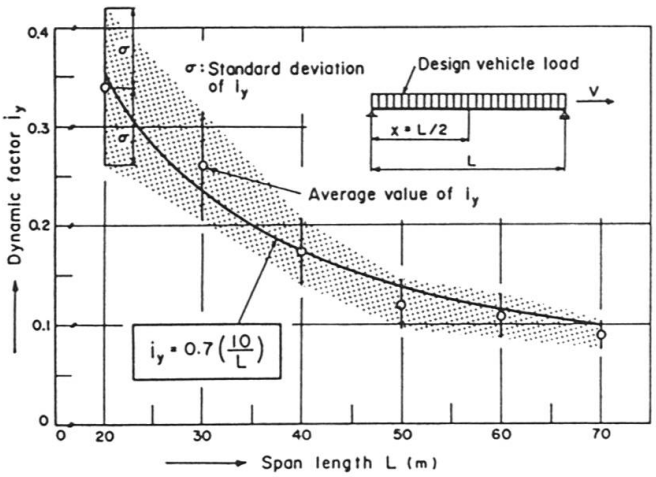

Fig.9 i_y of single-span steel girder bridges.

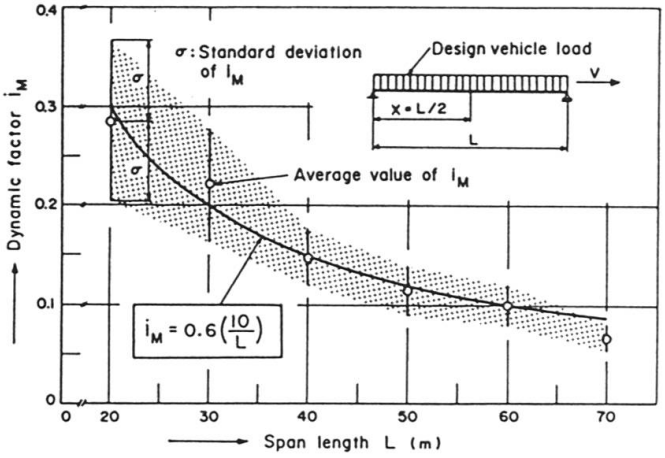

Fig.10 i_M of single-span steel girder bridges.

The L-20 (L-196 kN) load of highway bridges is assumed as the fully loaded condition of the span. However, the probability that such a condition will occur in normal traffic conditions is small. As shown above, the impact which will be added by such moving vehicles may also be small when a large number of vehicles are moving on the bridge. Although the response of bridges is calculated using the thirty sample functions of road surface roughness, it is not necessary to use the upper-limit value of each response of the thirty sample functions because the loading condition of the applied vehicle approaches the upper-limit value {11}. Therefore, the average value of the dynamic factors based on the thirty sample functions was taken in the calculation described below. Although the average value of i_y in Fig.9 changes with the span length, it decreases as the span is lengthened. Hence, the relationship between the average value and the span length was investigated. Then the dynamic factor i_y based on the deflection of single-span steel girder bridges could be approximated by the decreasing function of $i_y = 0.7(10/L)$ as shown in Fig.9.

On the other hand, Fig.10 shows the relationship between L and i_M based on the bending moment of single-span bridges. The symbols in this figure are the same as Fig.9. The dotted area and the standard deviation of i_M have the same trends described in Fig.9, but there is the relation of $i_M < i_y$ as was also found in the previous study {12}. Hence, the relationship between the average value of i_M and L was investigated, and then the dynamic factor i_M could be approximated by the decreasing function of $i_M = 0.6(10/L)$ as shown in Fig.10.

3.3 Dynamic factor of multi-span continuous steel girder bridges

3.3.1 Dynamic factor based on deflection

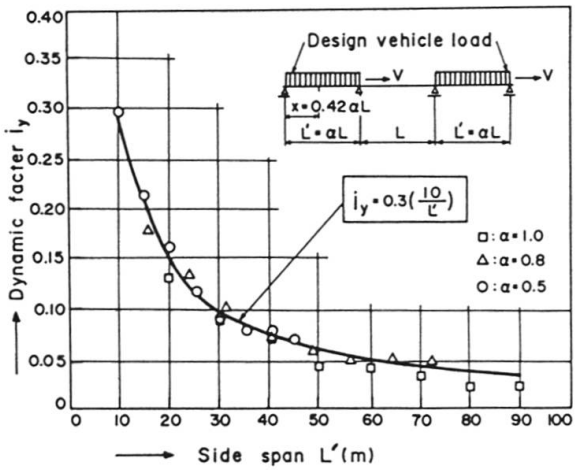

Fig.11 i_y at side span of three-span continuous steel girder bridges.

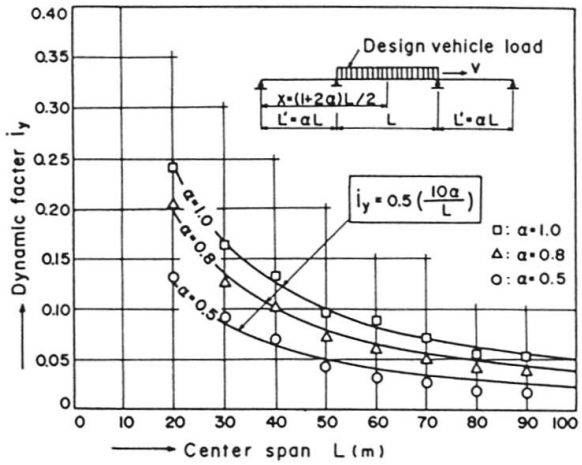

Fig.12 i_y at center span of three-span continuous steel girder bridges.

Fig.11 shows the relationship between the side span length L' and i_y of the three-span continuous bridges under the equivalent vehicle load line with the loading condition as described in Fig.8. α is the span ratio. Although the dynamic factor differs according to the span ratios, the dynamic factor with each span ratio decreases with the side span length. Hence, if the effect of the span ratio on the dynamic factor is omitted because the range of change of the dynamic factor and the span ratio is small, the dynamic factor can be approximated by a decreasing function of $i_y = 0.3(10/L')$ as shown in Fig.11.

Fig.12 shows the relationship between the center span length L and i_y in the same manner as Fig.11. The dynamic factor at α =1.0 is larger than that at α=0.5 because the maximum value of static deflection at α =1.0 is smaller than that at α =0.5 by the effect of both side spans. The dynamic factor is changed by the span ratios of the side span, but the dynamic factors for each span ratio decreases with the increase of the center span length. Hence, the effect of the span ratio on the dynamic factor was investigated, and then the dynamic factor was approximated by the function of $i_y = 0.5(10\alpha/L)$ as shown in Fig.12. It was found that the decreasing function of dynamic factor shown in Fig.12 has a larger value than that shown in Fig.11. The relation of the maximum dynamic factor to span length in three-span continuous bridges shown in Fig.11 and Fig.12 can be approximated by the decreasing function $i_y = 0.5(10/L)$.

3.3.2 Dynamic factor based on bending moment

Before going into the main argument, the relationship between i_y and i_M of continuous girder bridges which was investigated will be discussed. As a calculated example, Fig.13 shows the relationship between i_y and i_M of three-span continuous steel girder bridges under the equivalent vehicle load line of the loading condition as described in Fig.8. Although the dynamic factor of i_y and i_M differs with the span ratio and flexural rigidity, the i_M of the side span is generally smaller than the i_y as discovered in a previous study [13].

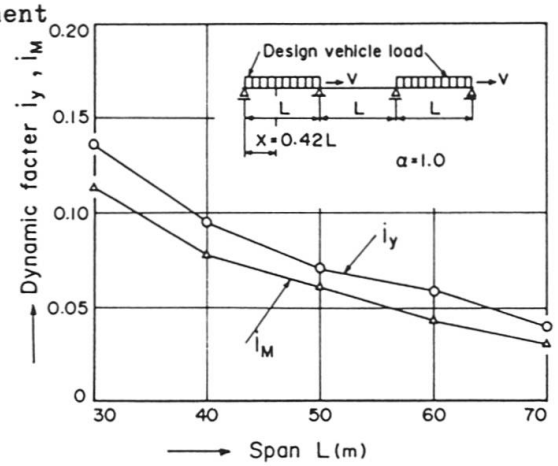

Fig.13 Relation between i_y and i_M at side span.

Figs.14-17 show the i_M of the multi-span continuous steel girder bridges under the equivalent vehicle load line of the loading condition as described in Fig.8. Fig.14 is the two-span continuous, Fig.15 is the three-span continuous, Fig.16 is the four-span continuous and Fig.17 is the five-span continuous bridge. The symbols L, L' and L'' indicate the span length where the impact factor in the design specification is calculated. $x_1 \sim x_5$ are the points where the calculation was made on the multi-span continuous bridge. The dotted line and the solid line show the dynamic factor at α =0.8 and α =1.0. From these figures, the dynamic factor decreases with the increase of the number of spans, and the value of i_M is scattered in the range of 0.2-0.02. In addition, all dynamic factors at the point $x_1 \sim x_5$ decrease with the increase of span length, and this tendency of i_M does not change even if the span ratio changes. When the relationship between the dynamic factor and the point of calculation was investigated, it was found that the i_M at the first-side span counted from the left-end support was the smallest for all continuous bridges, and i_M at the intermediate supports became larger at the support nearest the center of the bridge. The dynamic factor at other points is scattered in the range of that between the first-side span and the nearest support because the maximum value of the static bending moment at the first-side span becomes larger than that at the nearest support. In addition, it was found that the dynamic factor differs with the span ratio in Figs.14-17. For example, the dynamic factors at α =1.0 at the first-side span and at the second support counted from the left-end support becomes smaller than that at α =0.8. Finally, the dynamic factor differs with the span ratio because the maximum value of the bending moment is changed by the span ratio.

Although in this study the dynamic factor at each point of calculation of multi-span continuous bridges is calculated as described above, these dynamic factors are very complicated, and it is difficult to use them for the design of bridges. Therefore, taking into consideration the many years of design experience with the present specifications, it was decided to limit the dynamic factor calculation to each support point and a point between each pair of adjacent support points (mid-span points), as in conventional impact factor calculations. Also, it was decided to use only the maximum value of the dynamic factor calculated at the two sets of points. The resulting error may be small because the difference in the dynamic factors at the mid-span points and intermediate support points is not large as seen in Figs.14-17. Therefore, the relation of the maximum dynamic factor at mid-span points and intermediate support points to the number of spans and the span length was studied.

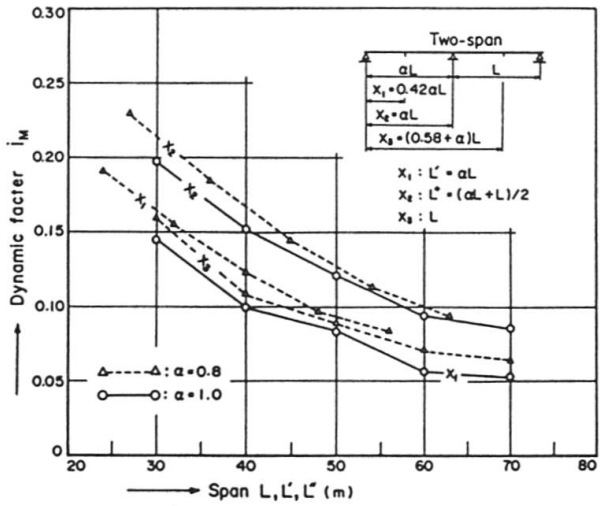

Fig.14 i_M of two-span continuous steel girder bridges.

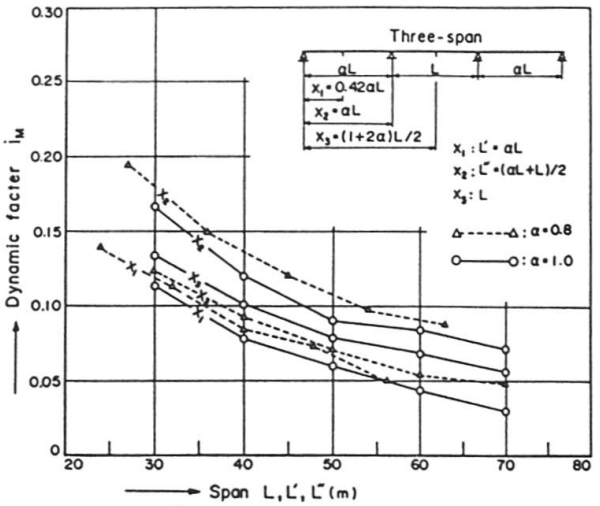

Fig.15 i_M of three-span continuou steel girder bridges.

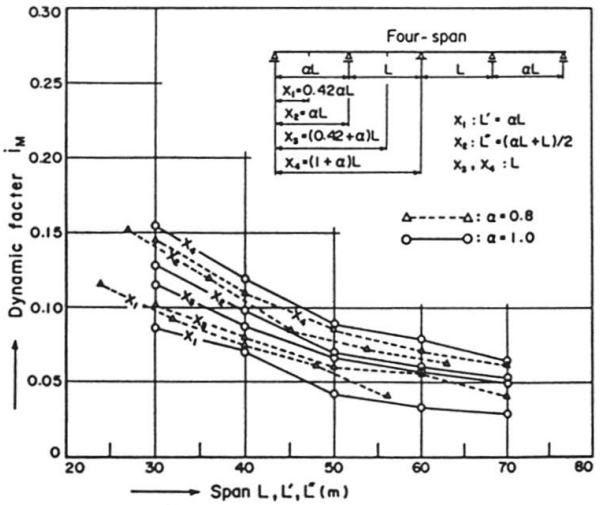

Fig.16 i_M of four-span continuous steel girder bridges.

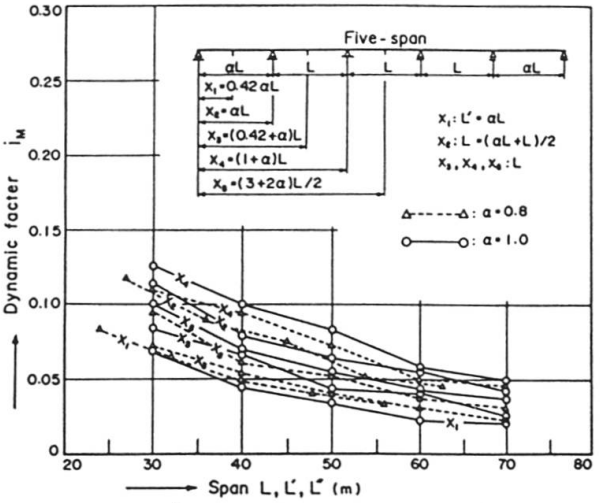

Fig.17 i_M of five-span continuous steel girder bridges.

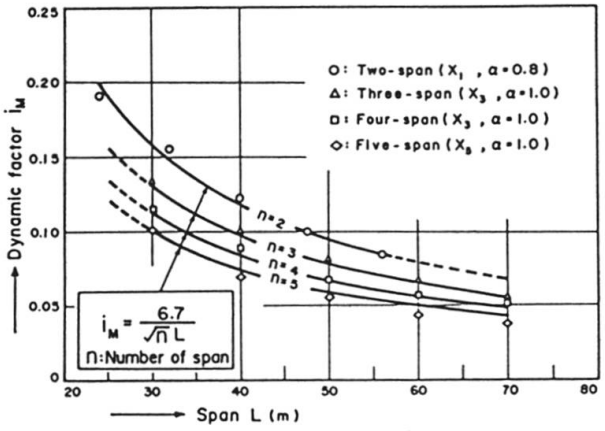

Fig.18 Maximum value of i_M at span point of multi-span continuous steel girder bridges.

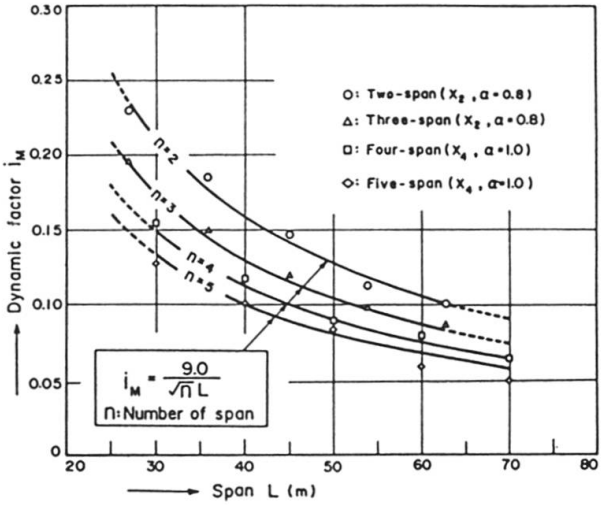

Fig.19 Maximum value of i_M at intermediate support point of multi-span continuous steel girder bridges.

Fig.18 shows the maximum value of i_M at each span point of multi-span continuous steel girder bridges. α and x_i in this figure show the span ratio and the point of calculation in the span point where the dynamic factor is largest in Figs.14-17, and n is the number of spans. The dynamic factor decreases with the increase of the number of spans, and the dynamic factor of each span also decreases with the increase of the span length. Finally, the dynamic factor at the span point of multi-span continuous steel girder bridges could be approximated by the decreasing function of $i_M = 6.7/(\sqrt{n}\ L)$ with two parameters: the span length and the number of spans as shown in Fig.18. The dynamic effects produced at each span point of the multi-span continuous girder bridges under moving vehicles could be expressed by a decreasing function. The effect of the number of spans evaluated by $1/\sqrt{n}$ can be understood by formula ρl in the normalized condition for the coefficient a_{nm} of vibration mode function shown in Eq.(3).

On the other hand, Fig.19 shows the maximum value of i_M at each intermediate support of multi-span continuous steel girder bridges. α and x_i in this figure show the span ratio and the point of calculation in the intermediate support where the dynamic factor is the largest in Figs.14-17. It is recognized that the dynamic factors have the same trends as described in Fig.18, but the dynamic factors at the intermediate support points are generally larger than those at the span point, as shown in Fig.18. Finally, the dynamic factor at the intermediate support point of multi-span continuous steel girder bridges can be approximated by the decreasing function of $i_M = 9.0/(\sqrt{n}\ L)$ in much the same way as the function illustrated in Fig.18, and the decreasing function is shown in Fig.19. The dynamic effects produced at each intermediate support point of multi-span continuous girder bridges under moving vehicles could be expressed by a decreasing function.

4. DYNAMIC FACTOR OF HIGHWAY STEEL GIRDER BRIDGES

4.1 Dynamic factor based on deflection

The expression "highway steel girder bridges" in this study will be used to designate both single-span and multi-span continuous steel girder bridges. Using the calculated results shown in Fig.9 and 12, Fig.20 shows the dynamic factor based on the deflection. The single-span bridge corresponds to n =1. In this figure, the impact factors of some major countries and the value suggested by the previous studies {14,15} are also illustrated to compare them with the calculated dynamic factors, although the analysis procedures differ. The dynamic factor of the three span continuous bridge is smaller than that of the single-span bridge by about 30%.

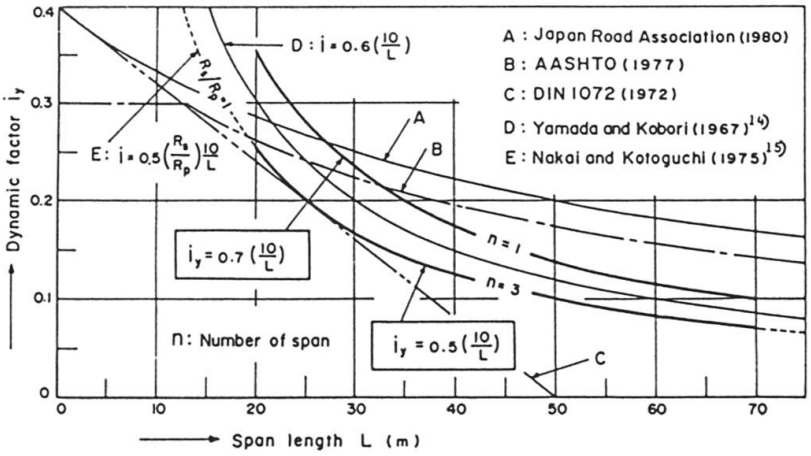

Fig.20 Dynamic factor based on deflection at mid-span of highway steel girder bridges.

In comparing the dynamic factor of a single-span with the impact factor of the curve A: $i = 20/(50 + L)$, the dynamic factor in the region where the span length is under 27 m is larger than given by curve A. Therefore, the Japanese design code underestimates the dynamic effect of such short span bridges. Generally, short span bridges have small natural periods. They are affected by the road surface roughness and by vehicles, two at the most, which vibrate with short periods. If a smooth road-surface is guaranteed, the dynamic factor can will be small. However, when the actual characteristics of road surfaces are considered {4,9}, it is necessary to estimate a large dynamic effect on short span bridges by a design live load because the dynamic response of such bridges is very sensitive to moving vehicles. The dynamic factor in the region where the span length is over 27 m is smaller than given by curve A, and the difference between such dynamic factors and curve A becomes larger when the span length increases. The Japanese design code will overestimate the dynamic effects of bridges with such span lengths. If the span length is longer, generally the ratio of the stress by live load to the stress by dead load becomes smaller. Therefore, a slight increase of live-load stress is not a serious problem in the design. For preference, the first step for a rational, economical design will be to make the dynamic factor as small as possible for bridges of long span length.

4.2 Dynamic factor based on bending moment

Using the calculated results shown in Figs.10 and 18, Fig.21 shows the dynamic factor based on the bending moment at the mid-span of highway steel girder bridges. In comparing the single-span with multi-span continu- bridges is smaller than that of the single-span bridge by about 21%, 30%, 44% and 50%, respectively. This is because in the calculation of the dynamic factor, the response of the bridge is directly affected by the increase of the total mass of bridge due to the increase of the number of spans. In addition, the dynamic factor in the region where the span length is over 20 m is smaller than curve A, but the dynamic factor at L =20 m exceeds curve A slightly. The difference between such dynamic factors and curve A becomes larger as the number of spans increases. Therefore, when the dynamic factor based on the bending moment is investigated in the same manner as that based on deflection, it will be necessary to make the dynamic factor as small as possible and to rationalize the design of such bridges.

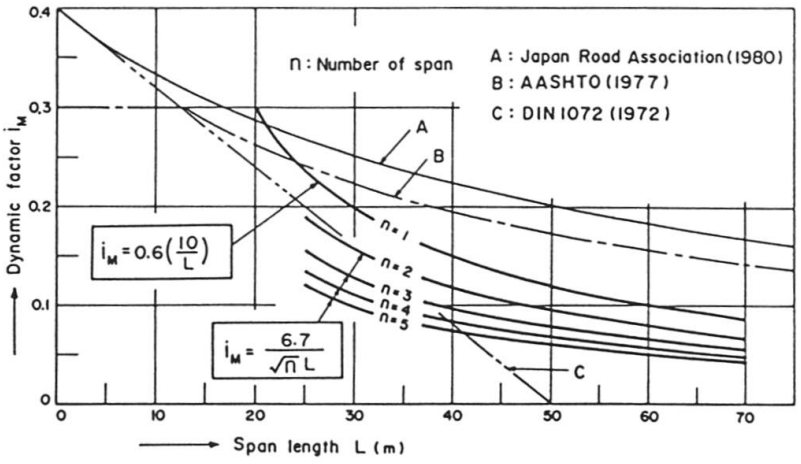

Fig.21 Dynamic factor based on bending moment at mid-span of highway steel girder bridges.

4.3 Design dynamic factor based on deflection and bending moment

From the investigated results for the dynamic factor described above, the design dynamic factor, i , which is based on the deflection and the bending moment, is given by a decreasing function with two parameters:

the span length, L , and the number of spans, n , as

$$i = i_1 \cdot i_2 \cdot i_3 \cdot i_0 \left(\frac{10}{L}\right) \leq 0.4, \quad 20 \leq L \leq 70 \text{ m} \qquad (17)$$

in which i_1 is the response parameter which shows either deflection or bending moment of bridge response when the dynamic factor is calculated, i_2 is the applied parameter which shows either mid-span or intermediate support, i_3 is the form parameter which changes according to whether the bridge is single-span or multi-span continuous, and i_0 is the standard dynamic factor. The actual values of these parameters are shown in Table 4.

Table 4 Design dynamic factor based on deflection and bending moment of highway steel girder bridges.

	$i = i_1 \cdot i_2 \cdot i_3 \cdot i_0 \left(\frac{10}{L}\right) \leq 0.4$, $20 \leq L \leq 70$ m	
i_1	Bending moment	1.0
	Deflection	1.2
i_2	Span	1.0
	Intermediate support	1.35
i_3	Single girder bridge	0.9
	Continuous girder bridge (n : number of span)	$1/\sqrt{n}$, $2 \leq n \leq 5$
i_0	Standard dynamic factor	0.67

Some added considerations to Eq.(17) are as follows: (1) The first consideration is the maximum value of i . As described in Fig.12, the dynamic effect of short span bridges is greatly affected by even one or two heaving moving vehicles. For such bridges, the maximum value of the dynamic factor can be considered to be the standard deviation plus the average value of the dynamic factor at L =20 m as illustrated in Figs.9 and 10. Therefore, the value of 0.4 is adopted as a practical value. (2) The second consideration is that the dynamic factor based on deflection at the intermediate support point of multi-span continuous bridges cannot be calculated because the deflection at the intermediate support point of such bridges is zero. The design dynamic factor based on deflection at the intermediate support point of multi-span continuous bridges in Eq.(17) is calculated using the calculated dynamic factor based on the bending moment.

4.4 Design dynamic factor based on bending moment

It is more desirable to use the bending moment than the deflection in the investigation of the impact factor,because the impact factor written in the design specification is used to mean the dynamic effect of the maximum stress caused by the design live load. Therefore, the design dynamic factor, i' , based on the bending moment of highway steel girder bridges is given in the same formula as Eq.(17), as follows,

$$i' = i_1' \cdot i_2' \cdot i_0 \left(\frac{10}{L}\right) \leq 0.4, \quad 20 \leq L \leq 70 \text{ m} \qquad (18)$$

in which i_1' is the applied parameter, i_2' is the form parameter, and i_0 is the standard dynamic factor. The actual values of these parameters are shown in Table 5.

Table 5 Design dynamic factor based on bending moment of highway steel girder bridges.

	$i = i_1' \cdot i_2' \cdot i_0 \left(\frac{10}{L}\right) \leq 0.4$, $20 \leq L \leq 70$ m	
i_1'	Span	1.0
	Intermediate support	1.35
i_2'	Single girder bridge	0.9
	Continuous girder bridge (n : number of span)	$1/\sqrt{n}$, $2 \leq n \leq 5$
i_0	Standard dynamic factor	0.67

5. CONCLUSIONS

The major conclusions of this study can be summarized as follows:

(1) The dynamic factor of short span bridges is greatly affected by the characteristics of road surface roughness and of moving vehicles, but the effects of these characteristics decrease with the increase of span length.
(2) The dynamic factor based on the bending moment is generally smaller than that based on the deflection.
(3) The dynamic factor at the intermediate support point is larger than that at the mid-span.
(4) The dynamic factor of multi-span continuous girder bridges is smaller than that of single-span girder bridges, and it decreases with the increase in the number of spans.
(5) The design dynamic factor based on both the deflection and the bending moment of highway steel girder bridges, including both single-span and multi-span continuous bridges, could be given by a decreasing function of the number of spans and the span length, as shown in Eq.(17), and the design dynamic factor based solely on the bending moment could be given by Eq.(18) in the same formula as Eq.(17).

Although the design dynamic factor obtained in this study is presented in a form more complicated than the impact factor in the present design specification, it can be calculated by a decreasing function of the dynamic effect of highway steel girder bridges, and the dynamic factor based on either the deflection and the bending moment can also be calculated. If the design dynamic factor is used as the impact factor, a useful and rational design can be obtained.

Recent studies have clearly shown the relationship between dynamic increment or dynamic load allowance and the first-flexural frequency of a bridge {16,17}. It is very important to investigate such relationships for the design of highway bridges. However, the impact factor written in design specifications is generally used to denote the dynamic effects of maximum stress caused by design live load. Therefore, in this study the analytical method using this design live load (L-20;L-196 kN) for vehicle load may be more practical and appropriate than that using other definitions. However, it is very difficult to investigate the dynamic factor by field tests using the design live load, because the design live load is considered the maximum load for the span, and it is basically different from normal load conditions. In

any case, hereafter it may also be necessary to investigate the precise definition of impact factor in the limit states design method (LSD) for highway bridges, and to investigate the relationship between impact factor and vibration limit on serviceability limit states in LSD because the level of daily-vehicle load is smaller than that of design live load.

APPENDIX I. --- REFERENCES

1. Hirai, I., A Dynamic Analysis of Continuous Beams on Elastic Supports, Proc. of the Japan Society of Civil Engineers (JSCE),No.104/1964.
2. Kato, M. and S. Shimada, Statistical Analysis on the Measured Bridge Vibration Data, Proc. of JSCE, No.311/1981.
3. Komatu, S. and M. Kawatani, Study on Dynamic Response and Impact of Cable-Stayed Girder Bridges under Moving Vehicles, Proc. of JSCE, No.275/1978.
4. Honda, H., Y. Kajikawa and T. Kobori, Spectra of Road Surface Roughness on Bridges, Proc. of ASCE, Vol.108, No.ST9/1982.
5. Hino, M., Spectra Analysis, Asakura Book Co., Inc., Tokyo, Japan, 1978.
6. Discussion and Closure of Reference {4}, Proc. of ASCE, Vol.109/1983.
7. Shinozuka, M. and T. Kobori, Fatigue Analysis of Highway bridges, Proc. of JSCE, No.208/1972.
8. Hirao, O. et al., Theoretical Vehicle Engineering, Sankaido Book Co., Inc., Tokyo, Japan, 1971.
9. Honda, H., Y. Kajikawa and T. Kobori, Roughness Characteristics at Expansion Joint on Highway Bridges, Proc. of JSCE, No.324/1982.
10. Page, J., Dynamic Forces Generated by Vehicles on Bridges, Transport and Road Resarch Laboratory Department of the Environment Crowthorne, IABSE Colloguium, Apr. 1975.
11. Ito, M. and Y. Osaka, Design Principle in Civil Engineering, Shokokusha Book Co., Inc., Tokyo, Japan, 1980.
12. Walker, W.H. and A.S. Veletsos, Response of Simple-span Highway Bridges to Moving Vehicles, Univ. of Illinois CESRS, No.272/1963.
13. Yoshimura, T., H. Hikosaka and T. Uchitani, Non-Stationary Random Response of Highway Bridges under A Single Moving Load, Proc. of JSCE, No.258/1977.
14. Yamada, Y. and T. Kobori, Dynamic Response of Highway Bridges due to Live Load by Spectral Analysis, Proc. of JSCE, No.148/1967.
15. Nakai, H. and H. Kotoguchi, Dynamic Response of Horizontally Curved Girder Bridges under Random Traffic Flows, Proc. of JSCE, No.244/1975.
16. Cantieni, R., Dynamic Load Testing of Highway Bridges, IABSE Proceedings, P-75/1984.
17. Billing, J. R. and R. Green, Dynamic Loading of Highway Bridges; Ontario, Final Report of 12th Congress of IABSE/1984.

APPENDIX II. --- NOTATION

The following symbols are used in this paper:

A = Parameter showing magnitude of impact at expansion joint;
a = Spectral roughness coefficient;

a_{nm} = Coefficient of vibration mode function;

c_i, c_i' = Damping factor at suspension and tire of vehicle;

EI = Bending stiffness of bridge;

g = Acceleration due to gravity;
i = Number of vehicles and design dynamic factor based on deflection and bending moment;
i' = Design dynamic factor based on bending moment;

i_M = Dynamic factor based on bending moment;

i_y = Dynamic factor based on deflection;

i_0 = Standard dynamic factor;

i_1 = Response parameter which shows either deflection or bending moment of bridge response when the dynamic factor is calculated;
i_2, i_1' = Applied parameter which shows either span point or intermediate support point;
i_3, i_2' = Form parameter which changes according to whether the bridge is single-span or multi-span continuous;

k_i, k_i' = Spring stiffness at suspension and tire of vehicle;

L, L' = Length of mid and end-spans;
l = Total span length of bridge;
$M(t,x)$ = Bending moment of bridge;

$M_{d,max}$ = Maximum value of dynamic bending moment;

$M_{s,max}$ = Maximum value of static bending moment;

m = Number of harmonic series;

m_i, m_i' = Sprung and unsprung mass of vehicle;

n = Number of harmonic series and spectral roughness exponent;
p = Natural frequency of bridge and vehicle at sprung mass;
p' = Natural frequency at unsprung mass of vehicle;

$q_n(t)$ = Generalized coordinate;

S = Interval distance of vehicles;

$S_r(\Omega)$ = PSD of road surface roughness;

t = Time from the moment when the moving vehicle comes on the bridge;
V = Speed of vehicle;
W = Weight of bridge;
x = Coordinate in right direction of bridge originated from left end-support of bridge;
x_i = Distance of left end-support to i support;

$y(t,x)$ = Deflection of bridge;

$y_{d,max}$ = Maximum value of dynamic deflection;

$y_{s,max}$ = Maximum value of static deflection;

z_i, z_i' = Vertical deflection of m_i and m_i';

$\dot{z}_i'(t_0^*)$ = Vertical velocity of unsprung mass at momentary time t_0^* passing expansion joint;

$z_r, \dot{z}_r(t)$ = Deflection of road surface roughness at time t ;
α = Span ratio ($\alpha = L'/L$);

γ_i = Weight ratio of the vehicles to standard vehicle weight in vehicle load line;
$\delta(t)$ = Dirac delta function;
ε_i = Parameter shown vehicle of number i "exist" or "not exist" on bridge;

λ_n = n -th frequency ratio of continuous girder bridge ($\lambda_n = \omega_n / \omega_{g1}$);

ρ = Bridge mass per unit span length;

$\phi_n(x)$ = Vibration mode function;

Ω = Roughness frequency;

ω_{g1} = First natural circular frequency of single-span bridge with span length of l ; and

ω_n = n -th natural circular frequency of continuous girder bridge.